Nonlinear response of membranes to pinning sites

R. Menes* and S. A. Safran
Department of Materials and Interfaces, Weizmann Institute of Science, Rehovot, 76100, Israel
(Received 26 September 1996)

Bound membranes respond to pinning sites by locally unbinding and overshooting their equilibrium spacing. This nonlinear response can lead to long-ranged interactions between these sites. We introduce a theory which incorporates bending elasticity, fluctuations, and intermembrane interactions to calculate the profiles of bound membranes subject to local pinning. This theory predicts several scaling regimes where the overshoot scales both with the pinning strength and site size. We also calculate the effective, membrane induced interaction between the sites, and predict aggregation properties. Aggregation and reversibility of pinning sites leads to interesting collective phenomena. [S1063-651X(97)01308-1]

PACS number(s): 68.10.−m, 87.22.Bt, 82.65.Dp

In the past decade there has been much interest in the physics of interacting membranes, and their adhesive properties [1]. Theoretical treatments of these systems have mainly focused on systems that interact uniformly through homogeneous interactions (i.e., van der Waals attraction), although there is clear evidence that local interactions dominate biological adhesion [2,3] and that even in homogeneous model systems local binding effects might be significant.

Bruinsma *et al.* [4] have considered the effects of local pinning on free, unbound membranes. They calculated the profiles of pinned unbound membranes and found an effective, logarithmic, membrane mediated interaction between pinning sites that they treated within a mean field calculation. In this paper we introduce a theory which treats systems of interacting, uniformly *bound*, membranes which also includes local binding or ''pinning'' effects, and calculate the membrane profiles and membrane mediated interactions which we consider within a virial expansion.

We focus on systems of membranes bound to an equilibrium intermembrane distance $\overline{h}$ by either attractive interactions or pressure. In addition to this uniform binding they are also subject to local adhesive patches (pinning sites) where the intermembrane distance is restricted to a value h_0 which is much smaller than the equilibrium value $\overline{h}$. We find that the overall binding of the membranes strongly affects the membrane profiles near a pinning site and hence dramatically changes the interaction between sites, which we find to be nonmonotonic.

The local pinning of interacting membranes, which is important both in the context of biological adhesion and in the understanding of more general membrane processes such as the unbinding transition [5,6], can be mesoscopically modeled by bilayer systems pinched together by laser tweezers [7]. The laser tweezer can trap the dielectric membrane material within a small region, and by trapping sections of both membranes induce an effective pinning site of micrometer size. Such experiments indicate that the elastic response of the membranes to pinning can be highly nonlinear, leading to local unbinding (overshooting) of the membranes in the vicinity of the pinch.

Biological adhesion is dominated by binding sites which locally pin one membrane to the other or to an adhesive surface [2,3]. Although these binding sites, which are composed of specific ''lock and key'' molecules, cover a limited area, and might have relatively weak bonding energies (they are reversible), they can have a rather strong effect on the embedding membranes, forcing the material in their vicinity to very close proximity. These local binding sites were observed to aggregate at certain stages in the process of adhesion [8]. The attractive interactions which cause aggregation can also include an effective, long-range, interaction induced by the membrane response to the strong pinning constraint.

In addition to the interesting biological systems that it addresses, the problem of pinning is also related to the unbinding transition of membranes [5,6]. This transition, which has been predicted by renormalization group techniques and has been reported experimentally, is driven by thermal fluctuations and attractions which induce collisions between neighboring membranes. Pinning sites, which model local collisions, and the membrane response to these sites can be useful in understanding the local collisions between fluctuating membranes and their role in this transition.

In a previous paper [7] we reported the results of an elastic model of interacting membranes which predicted the membrane profiles in the vicinity of a local pinning site. The model was introduced in the context of experiments which showed striking elastic response to laser pinching of interacting membranes. In Sec. I of this paper we introduce this model and briefly discuss its numerical solutions for profiles of membranes in the vicinity of pinning sites. In Sec. II we analyze the model using scaling methods and give a comprehensive picture of the scaling behavior of the system as it depends on the characteristics of the pinning site. Section III shows results pertaining to two or more pinning sites in fluid membranes, including their interaction and aggregation tendency.

I. ELASTIC MODEL FOR PINNED INTERACTING MEMBRANES

We consider systems of pairs of interacting membranes, or a membrane interacting with an adhesive substrate, subject to a local pinning site which effectively reduces the intermembrane distance at this site.

*Present address: Materials Research Laboratory, University of California, Santa Barbara, CA 93106.

Previous theoretical work [9,10] has addressed the problem of membranes weakly perturbed by inclusions. In the limit of small perturbations, linear response dictates that the membrane overshoots only slightly in the vicinity of the perturbation. In this paper, we address the more striking phenomena resulting from a strong perturbation effected by a strong pinning site. We also take into account, in an effective manner, the consequences of membrane curvature fluctuations. In a more fundamental treatment the fluctuations should be taken into account at the level of the partition function, since they renormalize, and can affect, all interactions in the system. However, this would make any analytical calculation difficult and we therefore introduce them into the free energy via effective, local interactions. Such an approximation is valid as long as we consider membranes in their bound state and do not pass through the unbinding phase transition where the fluctuations diverge [5]. A detailed calculation of the effects of a pinning site on undulation interactions between membranes and a justification for our local approximation is given elsewhere [11]; see also [12].

Our analysis of the pinning of two flat, bound, tensionless membranes is based on an interfacial curvature model [13] which takes into account both the bending energy [13,14] of the membranes and the effective intermembrane interactions which model the effects of thermal fluctuations [15]. The pinning enters through the boundary conditions we impose. As was emphasized above, we treat systems of homogeneously bound membranes. The binding can be induced either by attractive interactions or by pressure. The pressure can be either an osmotic pressure or an external pressure arising from the mechanical constraints of the system such as other nearby vesicles or the walls of an experimental cell. Although systems bound by pressure and systems bound by attractive interactions respond similarly to pinning sites there are some qualitative differences between these systems. Because the long-ranged pressure term dominates a decaying attraction, any pressure present in the system will dictate the qualitative behavior, and therefore the case of interest is that of membranes bound by pressure. In the following we will describe the theory for a system bound by pressure. For completeness we show in Appendix A the calculations and results for systems bound by attractive interactions.

The free energy has the form

$$F=\int\left(\frac{\kappa}{2}(\nabla^2 h)^2+V(h)+Ph\right)dS. \tag{1.1}$$

Here $h(\vec{r})$ is the local intermembrane distance, κ is the bending modulus, and P is the pressure. The integration is over the entire membrane area. The intermembrane interaction potential $V(h)$ is an effective repulsive interaction induced by the confinement of the thermal fluctuations. The loss in fluctuation entropy per membrane due to the proximity of the neighboring membrane produces an effective repulsion [16]:

$$V(h)=\frac{3\pi^2}{64}\frac{(k_BT)^2}{\kappa}\frac{1}{h^2}.$$

Although this interaction was initially calculated as an effective global interaction between membranes with average distance h, recent calculations indicate that there are cases when this interaction can also be taken as a local interaction, even when the membranes are not parallel, so long as the effects of the pinning vertices are kept small by relatively large angles or stiff membranes [11]. Furthermore, scaling arguments recently proposed by Netz [12] indicate that in systems of free membranes locally pinned to a surface, introducing fluctuation effects at the partition function level gives similar results to those obtained by simply including the local version of the Helfrich interaction [4].

The minimum energy configuration of a membrane near a pinning site is given by solving the fourth order, nonlinear Euler-Lagrange equation which results from the minimization of the free energy [Eq. (1.1)] with respect to the profile $h(\vec{r})$:

$$\kappa\nabla^4 h(r)+\frac{dV}{dh}+P=0. \tag{1.2}$$

Far from the pinning site, the membrane profile is flat and given by the balance of dV/dh and P. In systems bound by pressure this means that $P\propto 1/\overline{h}^3$ and the free energy density in this region is $F_0\propto 1/\overline{h}^2$, where $\overline{h}$ is the equilibrium intermembrane distance. For axially symmetric systems, the equation is solved near the pinning site with two boundary conditions at the edge of the pinch, $r=r_0$: The first is that at the pinning site the membranes are forced to maintain a distance $h_0<\overline{h}$; the second condition is that of a free slope which means that the membranes minimize their free energy with respect to the slope at the boundary. This is equivalent to imposing $\nabla^2 h|_{r=r_0}=0$ (i.e., zero curvature at the edge of the pinning site). An alternative view of this boundary condition is given by the observation that the membrane profile must rise outward from the pinning area but returns asymptotically to the equilibrium spacing. Therefore there must be an inflection line around the pinning site where the curvature vanishes. One can choose this line as the effective edge of the pinning site and define its strength through the intermembrane spacing at this line, h_0. At infinity the spacing decays back to the equilibrium value $\overline{h}$, which defines the remaining boundary conditions.

Previous work [9,10] treated the limit $h_0\approx\overline{h}$, where Eq. (1.2) can be linearized [i.e., $V(h)+Ph$ are approximated by a quadratic form around the minimum energy state $h(\vec{r})=\overline{h}$]. In this limit the Euler-Lagrange equation for the minimum of the free energy is easily solved in terms of Bessel functions. These are oscillatory decaying solutions which exhibit an overshooting response to the pinning. In this limit, however, the overshoot is invariably small: it is proportional to $(\overline{h}-h_0)/\overline{h}$, which is the small parameter in the linearization.

In the nonlinear case where $h_0\ll\overline{h}$, the pinning is strong and the membrane response is striking. The repulsive interaction in the vicinity of the pinch is strong, leading to a large positive slope [17] and thus a strong overshooting response. In order to minimize the curvature energy the profile oscillates [9,10]. The strong overshooting response to the small intermembrane distance at the pinning site is clearly demonstrated in Fig. 1 where we show membrane profiles for a system bound by pressure with relatively strong pinning sites

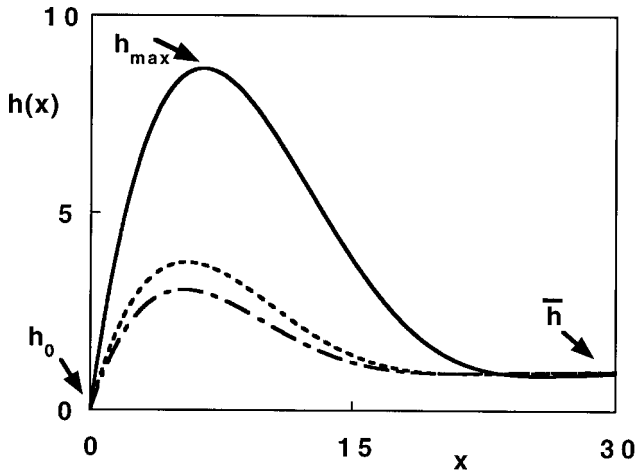

FIG. 1. Numerical profiles for a pinch of $r_0 \sim 1$ and several pinching strengths. $h_0 = 1 \times 10^{-4}$—solid curve, $h_0 = 3 \times 10^{-4}$—dotted curve, and $h_0 = 1 \times 10^{-3}$—dashed curve. The membrane height and the distance from the pinch are both measured in units of the equilibrium intermembrane distance $\overline{h}$. The curves were calculated with the realistic rigidity, $\kappa \sim 15 k_B T$.

and relatively small area ($h_0/\overline{h} = 10^{-4}$–$10^{-3}$ and $r_0/\overline{h} \simeq 1$). The overshooting response can be suppressed by lower order gradient terms such as surface tension. Membranes under relatively high surface tension will not exhibit the oscillations and overshooting characteristic of systems governed by curvature energy. Rather, their profiles will decay monotonically in order to minimize area [18]. In our discussion we limit ourselves to systems of negligible surface tension, such as μm size vesicles, where curvature rather than area must be minimized [19].

II. SCALING BEHAVIOR OF THE PINNED MEMBRANE

In addition to the dimensionless, small, parameter $\sqrt{T/\kappa}$ which scales all membrane slopes, there is a natural length scale in this problem which is the equilibrium intermembrane distance $\overline{h}$. We use $\overline{h}$ to scale all other lengths in the problem. We characterize the membrane profile by the maximum height it reaches in the overshooting region, h_m, and the overall horizontal extent of the overshooting ''bump,'' W (see Fig. 2). These two length scales are determined by the physics introduced by two other important length scales: The area of the site, r_0^2, and the intermembrane distance in the pinning region, h_0. As indicated in the preceding section, the strength of pinning is modeled by $h_0/\overline{h}$. These two length scales are the parameters that determine the membrane profile.

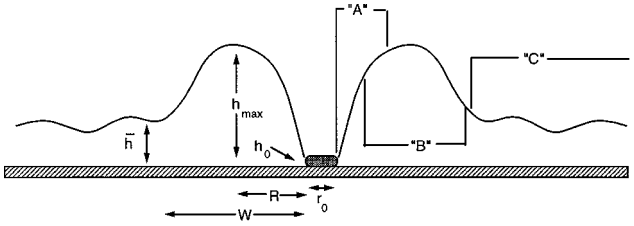

FIG. 2. Schematic profile of a membrane near a pinning site. Region A is the strongly repulsive region near the pinch, region B is the overshooting region, and region C is the equilibrium state. The overshoot reaches a maximum height denoted by $h_{\max}$ and extends in the horizontal direction a length W. The pinning site is characterized by the pinning distance h_0 and the pinning area r_0^2.

By minimizing the free energy of the pinched system with respect to h_m we can formulate scaling relations for the overshoot profile. We find that the system has several scaling regimes depending on both $h_0/\overline{h}$ and $r_0/\overline{h}$. The different scaling regimes are relevant to different systems depending on the magnitude of h_0 and r_0.

The scaling behavior of systems dominated by pressure and those dominated by attraction are different and therefore we give separate treatments for these two types of systems. In the following, we treat one scaling regime for systems dominated by pressure, and in Appendix A we treat the equivalent regime in systems dominated by attractions. In Appendix B we outline the full treatment of all regimes for both systems bound by pressure and systems bound by attractions.

The first scaling law for W is obtained by analyzing the free energy and Euler-Lagrange equation [Eqs. (1.1) and (1.2)] in the region of the strong overshooting bulge, away from the actual pinning site and before the membrane returns to its equilibrium position. This is region ''B'' of Fig. 2. In this region, the size and strength of the pinning site are not important but the long-range behavior of the binding interaction is: The term dV/dh is negligible so that the pressure term and curvature term are left to balance each other. A dimensional analysis of this balance indicates that

$$W/\overline{h} \sim (h_m/\overline{h})^{1/4}. \tag{2.1}$$

This law is correct for all h_0, r_0, and it describes the shape of the overshooting bump but does not determine its size. The size of the overshoot depends on the pinning through its area and strength. Therefore to determine the overshoot strength we must look at the profile very close to the pinning site. It is in this region that the differences between the various limits arise. For the sake of clarity, we will give, in the following, a detailed description of one scaling regime, the quasi-one-dimensional limit, while the scaling relations for the other limits are discussed in Appendix B and briefly summarized at the end of this section. In the limit where the pinning area is relatively large ($r_0/W \gg 1$) the free energy integrals can be approximated by one-dimensional integrals and the system's response to pinning is independent of r_0.

To determine the overshoot height we calculate (in the spirit of a variational approximation) an approximated form of the free energy of the system and minimize it with respect to h_m. In doing so we will use the already known form of the scaling law for W [Eq. (2.1)]. First we consider the profile very close to the pinning site. In this region (region ''A'' of Fig. 2) the pressure term is negligible and we approximate the solution to Eq. (1.2) by a conelike profile:

$$h(\vec{r}) = h_0 + \alpha(|\vec{r}| - r_0).$$

This solution does not satisfy the free slope boundary condition at the pinning site so it should be modified at the boundary. However, as can been seen from the profiles in Fig. 1, it

is a good approximation for the close vicinity of the boundary, and sufficient for the scaling analysis. Using this linear solution we can easily calculate the free energy density which in the one-dimensional limit takes the form

$$\langle F\rangle_A \propto \left(\frac{T^2}{\kappa}\right)\int_{r_0}^{R+r_0}\frac{1}{h(x)^2}dx \propto \frac{r_0}{\alpha}\left(\frac{T^2}{\kappa}\right)\int_{h_0}^{h_m}\frac{1}{h^2}dh \propto \left(\frac{T^2}{\kappa}\right)\frac{Wr_0}{h_0 h_m}. \tag{2.2}$$

This result should be added to the free energy density of region ''B'' (since the free energy in region ''C'' is constant and independent of h_m it does not contribute to the minimization and therefore is omitted from this calculation) which we find by inserting the first scaling relation in the pressure and curvature terms. In systems bound by pressure we find

$$\langle F\rangle_B \sim Wr_0 P(\overline{h})h_m \sim Wr_0\frac{T^2}{\kappa}\frac{h_m}{\overline{h}^3}. \tag{2.3}$$

Now we minimize the sum of these two terms, $\langle F\rangle_A+\langle F\rangle_B$, with respect to h_m to find the overshoot which has lowest energy. This yields the relation

$$\frac{h_m}{\overline{h}} \sim \sqrt{\frac{\overline{h}}{h_0}}. \tag{2.4}$$

The two relations, Eq. (2.1) and (2.4), describe the overshoot profile for a system bound by pressure in the limit of a large area pinning site. In Appendix A we develop the equivalent relations for systems dominated by attractions.

Numerical solutions of Eq. (1.2) with the boundary conditions mentioned in the preceding section confirm these scaling relations. In the case of the $r_0\to\infty$ limit we can solve the one-dimensional version of Eq. (1.2) to find profiles of overshoots of various sizes. In Fig. 3 we show the results of these one-dimensional solutions for the membrane minimum energy profiles. We show h_m and W as a function of $h_0/\overline{h}$ for systems bound by pressure as well as for systems bound by attractive interactions. The numerical results confirm the scaling laws obtained for this regime which are indicated by the solid lines in this figure.

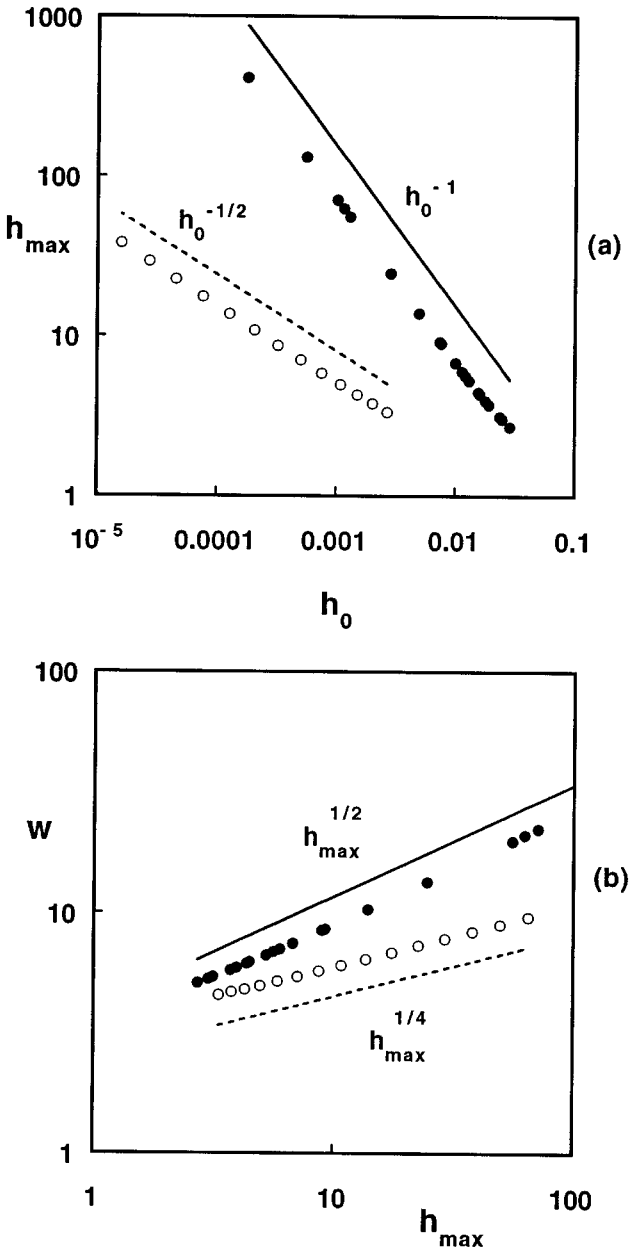

FIG. 3. (a) Maximum intermembrane separation (overshoot) as a function of the intermembrane distance h_0 at the pinching point, both for the pressure case (empty circles) and the interaction case (filled circles). (b) Width of overshooting region as a function of the overshoot. The graphs show the scaling laws in the one-dimensional limit discussed in the text (i.e., $r_0\to\infty$).

Other scaling regimes

The one-dimensional limit is probably the most physically interesting limit because it may correspond to a patch of many aggregated sticking sites in biological adhesion and is also most appropriate for the random collisions in fluctuating membranes, since very small contact regions are unfavorable with respect to curvature energy. However, numerical solutions of the two-dimensional Eq. (1.2) (for pinning sites which were relatively small or weak) show that there are other scaling regimes which qualitatively differ from the one-dimensional limit.

Using the same considerations and arguments presented for the one-dimensional limit one can calculate the relevant scaling relations for other regimes of the problem. The results of these scaling arguments for all the limits are calculated in Appendix B and summarized in Table I and Fig. 4 where the scaling regimes are shown as a function of the intermembrane distance at the pinning site h_0 and the pinning area r_0. The boundaries of the different regimes are approximate and the corresponding scaling behavior is only accurate deep inside the regimes. The results show that there are three regimes for each case (both the case of systems dominated by pressure and systems dominated by attractions). For large pinning area, we find the one-dimensional regime where the overshoot height h_m scales inversely with a power of the pinning strength h_0; for smaller pinning areas we find the intermediate regime which scales with a weaker power, and also scales with the area through r_0. For even smaller pinning areas the scaling is even weaker and the

TABLE I. Scaling regimes and results both for systems bound by pressure and systems bound by attractive interactions.

Pressure	Regime	$\frac{W}{\bar{h}} \sim \left(\frac{h_m}{\bar{h}}\right)^{1/4}$
I	$\frac{r_0}{\bar{h}} \gg \left(\frac{\bar{h}}{h_0}\right)^{1/8}$	$\frac{h_m}{\bar{h}} \sim \sqrt{\frac{\bar{h}}{h_0}}$
II	$\frac{h_0}{\bar{h}}\left(\ln\frac{\bar{h}}{h_0}\right)^{4/3} \ll \frac{r_0}{\bar{h}} \ll \left(\frac{\bar{h}}{h_0}\right)^{1/8}$	$\frac{h_m}{\bar{h}} \sim \left(\frac{r_0}{h_0}\right)^{4/9}$
III	$\frac{r_0}{\bar{h}} \ll \frac{h_0}{\bar{h}}\left(\ln\frac{\bar{h}}{h_0}\right)^{4/3}$	$\frac{h_m}{\bar{h}} \sim \left(\ln\frac{\bar{h}}{h_0}\right)^{1/3}$
Attraction	**Regime**	$\frac{W}{\bar{h}} \sim \sqrt{\frac{h_m}{\bar{h}}}$
I	$\frac{r_0}{\bar{h}} \gg \sqrt{\frac{\bar{h}}{h_0}}$	$\frac{h_m}{\bar{h}} \sim \frac{\bar{h}}{h_0}$
II	$\frac{h_0}{\bar{h}}\left(\ln\frac{\bar{h}}{h_0}\right)^{3/4} \ll \frac{r_0}{\bar{h}} \ll \sqrt{\frac{\bar{h}}{h_0}}$	$\frac{h_m}{\bar{h}} \sim \left(\frac{r_0}{h_0}\right)^{2/3}$
III	$\frac{r_0}{\bar{h}} \ll \frac{h_0}{\bar{h}}\left(\ln\frac{\bar{h}}{h_0}\right)^{3/4}$	$\frac{h_m}{\bar{h}} \sim \sqrt{\ln\frac{\bar{h}}{h_0}}$

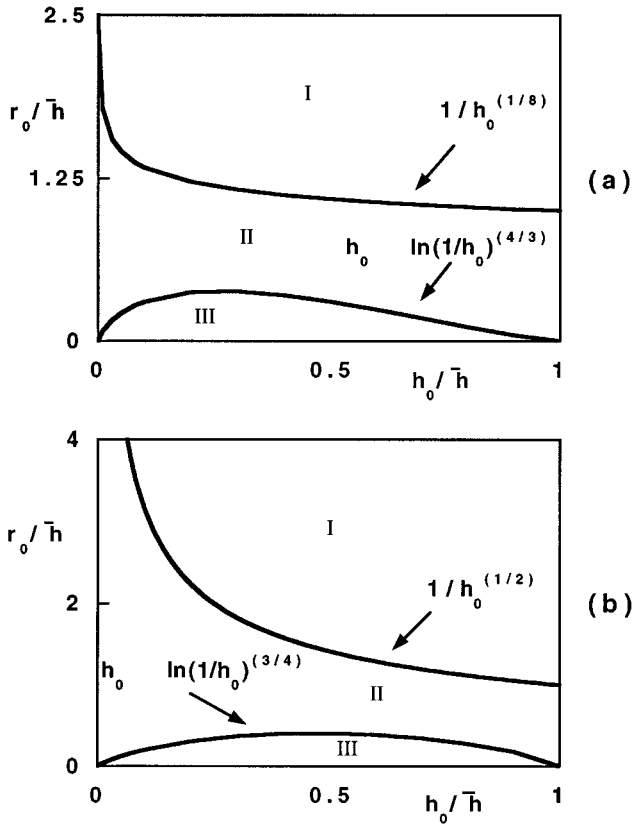

FIG. 4. (a) Scaling regimes as a function of pinning strength h_0 and pinning area r_0^2 for a system bound by pressure. (b) Scaling regimes as a function of pinning strength h_0 and pinning area r_0^2 for a system bound by attractive interactions. Both types of systems show three scaling regimes which differ by their scaling strength from the strongest quasi-one-dimensional regime (I) to the weakest logarithmic regime (II) characterized by small pinning area. The figures also show the functional forms of the borders between regimes. The scaling relations are detailed in Table I.

overshoot size is a logarithmic function of the intermembrane distance at the pinning site h_0. In all three regimes the overshooting increases as $h_0 \to 0$; the strength of scaling increases as the area of the pinning site increases, as would be expected for a perturbation in two dimensions. In the one-dimensional regime and the small r_0 limit the profiles are essentially independent of r_0 while in the intermediate regime the overshoot scales as a power law with r_0.

It is important to note that the scaling relations summarized in Fig. 4 and Table I are strongly dependent on the exact form of the repulsive undulation interaction near the pinning site. We have shown elsewhere that also for wedge-like geometries, such as are produced by the membrane response to the pinning, the undulation repulsion has the same inverse square form [11]. However, if the pinning brings the membranes to very close distances (10–100 Å) other, stronger, molecular interactions might become prominent and the scaling relations may change accordingly. Although the scaling laws and the regime boundaries are expected to change we still expect the main features of our analysis to remain (i.e., a quasi-one-dimensional regime which does not scale with the pinning area, another regime where the overshooting scales both with h_0 and r_0 and one or two regions of relatively weak pinning where the scaling is at most logarithmic).

III. INTERACTIONS OF SEVERAL PINNING SITES

In physical systems that include pinning sites, the collective behavior of these sites is important to the observed phenomena [8,9]. Both in biological adhesion and in the unbinding transition, pinning sites (''lock and key'' molecules in adhesion and random local collisions in the unbinding transition) can be treated as particles in a two-dimensional fluid (i.e., they are mobile in the membranes and not spatially pinned). The number of particles is not conserved: The ''lock and key'' molecules can open and close, and random collisions can fluctuate away and back again.

In a full treatment of a system of many pinning sites the reversibility of the sticker should be taken into account when calculating the membrane profiles. However, a complete description of the interplay of the sticker energetics and the membrane response to the stickers would be difficult to treat and therefore we chose to treat this problem perturbatively. Essentially we assume that the stickers have a narrow spectrum of binding energy and that we can model this binding with one set of boundary conditions. This is the assumption that led to the calculations in Secs. I and II. We also assume that although the stickers are reversible they are relatively stable so that we can ask questions about bond formation and aggregation and equilibrium phases without worrying that these effects may also in turn affect the profiles and resulting interactions.

In this section we show on a qualitative level how the membrane conformations between sticker sites generate an effective interaction between the stickers which determines

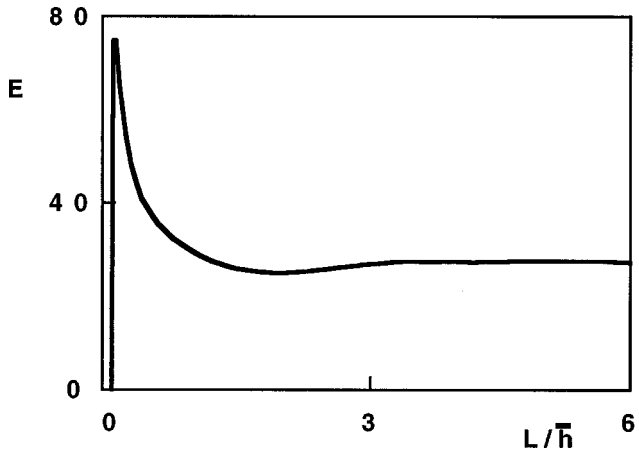

FIG. 5. Energy of two pinning sites as a function of the distance L between them, calculated numerically in the one-dimensional limit for pinning sites of strength $h_0/\overline{h}=0.012$, and $\kappa=15k_bT$. L is in units of the equilibrium intermembrane distance $\overline{h}$ and the free energy is in units of k_BT.

their aggregation properties and thus the stability of reversible stickers. Since the membrane induced interactions are of much longer range than the direct interactions, they dominate the aggregation at long distances. We begin by calculating this effective interaction energy between two sticking sites and show how this affects the aggregation properties and bonding stability.

Molecular pinning sites can interact via direct interactions (such as van der Waals attraction or other short-range interactions) and via effective interactions induced by the surrounding membranes [4,20]. The strong membrane response to a pinning site affects the free energy of the system and induces interactions between the pinning site and any other nearby inclusions or boundaries in the system, including other pinning sites. These effective interactions can be relatively long ranged because they scale with the length scale of the deformations, $\overline{h}$. Their range is the same, more or less, as the range of the overshooting bulge which can be large for strong pinning. (In the preceding section we showed how the size of the overshoot scales with the pinning strength.) Because the effective membrane induced interaction is longer ranged than the direct interactions, they are dominant in the aggregation of the sites.

In Fig. 5 we show the effective interaction between two pinning sites as a function of their distance (i.e., the difference in free energy between two pinning sites a distance L apart, and two coalesced pinning sites). The interaction was calculated numerically in the one-dimensional limit. In this system the pinning area is effectively infinite and the pinning strength is relatively strong ($h_0/\overline{h}=0.012$).

The system shows a shallow metastable state while the global minimum of the interaction is reached only when the pinning sites coalesce. The metastable state is reached when the two sites are separated by a distance which is of the order of the overshoot size, and is optimal for the curvature energy of the membrane. Once the pinning sites are closer than this geometrically optimal distance the curvature energy rises steeply, resulting in a high energy barrier. The barrier height is determined by the intersection of the curvature energy of this system with the energy of a system of two pinning sites with a *flat* membrane between them. In the latter case the interaction energy consists only of the strong repulsive Helfrich term and no curvature energy. This interaction is zero when the two pinning sites coalesce and rises rapidly with their separation, as can be seen in Fig. 5.

Although the interaction shown in Fig. 5 was calculated in the extreme one-dimensional limit we expect the main features of the effective membrane induced interaction, i.e., the metastable state and its position, the high barrier and global minimum at coalescence, to remain relevant in the two-dimensional systems. These features are characteristic of initially bound membranes. Work on unbound systems indicates that the interaction between sites rises logarithmically with their distance and never levels off [4]. This interaction was treated within a mean field analysis indicating no critical aggregation behavior. In the following we model the intersite interaction by a square well potential and use a virial-like expansion to find the critical behavior.

To treat systems of many pinning sites and the problem of aggregation we must also consider entropy effects. In addition to the translational entropy of the pinning sites, entropy also affects the membrane mediated interaction via thermal curvature fluctuations which are a dominant factor in the membrane response to pinning. The free energy per unit area of a system of many adhesion sites with concentration n has the approximate form [14]

$$f(n)=-\frac{1}{2}bn^2+T[n\ln n+(1-n)\ln 1-n], \qquad (3.1)$$

where the first term is an effective second virial coefficient and the second term is the entropy of mixing in a lattice gas model for the pinning centers. We can use this form of expansion if we assume the stickers are relatively dilute and because the interaction has a finite range which is of the order of the range of the membrane's response to the sticker, W.

Using the scaling arguments presented in Sec. II we can easily construct a simple model for the thermal aggregation properties. For simplicity we consider a potential well approximation for the interaction shown in Fig. 5. The depth of the well is proportional to the energy difference between two coalesced sites and two distant sites, while the well width is the horizontal length scale, W. The interaction coefficient for the attraction then consists of the product of the depth and width of the well: $b(T)\propto[F(l=0)-F(l=\infty)]W$. The energy of two coalesced sites is equal to the energy of one site with doubled area (this area factor is not significant because it changes the energy only by a numerical factor) and therefore

$$b\propto[F(1\text{ site})-F(2\text{ sites})]W\sim -F(1\text{ site})W.$$

The energy of a pinning site was calculated in Appendix B for all the scaling regimes. From Eq. (B1) we can estimate the interaction in the three regimes (pressure binding only) for a two-dimensional system. Each regime has a different interaction coefficient:

$$b \sim T\left(\frac{\overline{h}}{h_0}\right)^{3/4}, \quad \text{regime I,} \tag{3.2a}$$

$$b \sim T\left(\frac{r_0}{h_0}\right)^{2/9}, \quad \text{regime II,} \tag{3.2b}$$

$$b \sim T\sqrt{\ln\frac{\overline{h}}{h_0}}, \quad \text{regime III,} \tag{3.2c}$$

where the regimes I, II, and III are defined in Fig. 4 and Table I. The temperature dependence is analogous to that of entropic solids, such as polymeric gels, which condense upon heating. In these systems, the attraction between the aggregating objects is an effective manifestation of thermal fluctuations in the media connecting these objects. In our case the thermal fluctuations of the membrane curvature induce a strong repulsive response between the *membranes* near the pinning site which costs curvature energy and therefore induces attraction between the *sites*. The higher the temperature, the stronger the membrane repulsive response and the resulting attraction between sites increases.

Although the interaction coefficients in the three regimes scale differently with the pinning strength, there is a common trend. As the intermembrane distance h_0 at the pinning site is decreased, the interaction increases and eventually the stickers will phase separate. In the lattice gas model this happens when $b/T \geqslant 4$. Since b/T is temperature independent there will be no critical behavior as the temperature is varied, but there will be a transition as the intermembrane pinning distance h_0 and the pinning area r_0^2 are varied. As was noted at the end of the preceding section, the quantitative exponents of the scaling laws depend strongly on the form of the repulsion near the pinning site and therefore will also affect the aggregation properties.

The implications of these qualitative results to nonuniform adhesion (early stage biological adhesion) and to the unbinding transition must also take into account the reversible nature of the pinning sites. With the exception of designed model systems, most individual adhesion sites are formed by reversible stickers [3]. The stickers will bond and unbond as a function of temperature and the bonding energy and as a response to the pulling of the membrane.

The uniform binding of the membranes via either pressure or other attractive interactions increases the probability for membrane patches to approach, thus increasing the probability for a pinning site to form. The probability of a lock and key bond to form is proportional to the concentration of key molecules, n_k, the concentration of lock molecules, n_l, a Boltzmann factor for the lock and key bonding energy, $\exp(\epsilon/k_BT)$, and the probability that the membrane patches are closer than some minimum distance a_0 needed for a bond to form, $P(h \leqslant a_0)$. When confined, fluctuating membranes tend to fill space, thus the probability to find a patch of membranes at some distance h is more or less constant and therefore inversely proportional to the intermembrane distance $\overline{h}$. Hence, the probability for two membrane patches to approach closer than some minimum value a_0 required for a sticker to form is proportional to the ratio $a_0/\overline{h}$. Consequently, the sticking probability has the form

$$P \propto n_k n_l \exp\left(\frac{\epsilon}{k_BT}\right) a_0/\overline{h}.$$

The average distance between the fluctuating membranes does not have to be smaller than a_0 for a significant sticking probability.

The most interesting aspect of the reversibility of the stickers is its interplay with their aggregation properties. A sticker which is stuck within an aggregate has increased ''stickiness'' because the effects of the surrounding pulling membrane are screened by the neighboring stickers; in addition it cannot gain translational entropy by unbonding. In effect, the bonding energy of stickers within an aggregate is increased by the membrane deformation energy of an isolated sticker. This energy was shown to depend on the pinning strength through $h_0/\overline{h}$. On the other hand, the reversibility of the stickers stabilizes aggregates with respect to dispersed states for the same reasons that aggregation stabilizes the bonds: Isolated stickers have a shorter lifetime than stickers within an aggregate. The interplay of aggregation and sticker reversibility may be essential to the interesting collective phenomena in both biological adhesion and the unbinding transition.

ACKNOWLEDGMENTS

This work was motivated by experiments performed by Roy Bar-Ziv and Elisha Moses and has greatly benefited from their ideas. We are grateful to Phil Nelson and especially Phil Pincus for useful discussions. We acknowledge the support of the Israel Science Foundation administered by the Israel Academy of Sciences and Humanities.

APPENDIX A: MEMBRANES BOUND BY ATTRACTIVE INTERACTIONS

In this appendix we briefly describe the calculations and results for systems bound by attractions corresponding to Secs. I and II for the pressure case.

In systems bound by attractions the pressure is negligible and binding is the result of the balance of the repulsive and attractive interactions. The interaction term $V(h)$ can also include microscopic attractive interactions (e.g., van der Waals [21]). The attractive interactions are renormalized [5] by the thermal fluctuations of the membranes which cause the intermembrane distance to fluctuate; the effective attraction can be relatively long ranged. This is due to the fact that even when the average membrane separation is large, the fluctuations produce regions which are close and therefore interact strongly. One model for the attraction uses a Flory type argument [22] to write

$$V_a(h) \sim -\frac{1}{h}.$$

We studied several such effective interactions [23] and found that, qualitatively, the system is not sensitive to the exact form and range of the effective attraction so long as it decays to zero when the intermembrane distance $h(\vec{r})$ goes to infinity.

In systems that are dominated by an attraction such as $V_a=-v_a/h$ the equilibrium intermembrane distance is given by

$$\overline{h}\propto\frac{1}{v_a} \quad \text{and} \quad F_0=-\frac{v_a}{2\overline{h}^2} \tag{A1}$$

Solving the Euler-Lagrange equation [Eq. (1.2)] for such a system with the same pinning boundary conditions produces profiles that are indistinguishable from those shown in Fig. 1 for the pressure case. However, we find that this case exhibits different scaling relations than the pressure case.

The steps leading to the calculation of the scaling relations of systems dominated by attractions are similar to those dominated by pressure. Starting with region B of Fig. 2 we see that the only non-negligible term in the free energy is the curvature energy. The scaling law for the horizontal extent of the overshoot, W, is found to be

$$W/\overline{h}\sim\sqrt{h_m/\overline{h}}. \tag{A2}$$

The second relation is derived exactly as in the case of pressure dominated systems. The free energy density in region A is the same as in the case of pressure dominated systems [Eq. (2.2)] and the energy density in region B [Eq. (A2)] is found to be a constant dependent only on the equilibrium intermembrane distance $\overline{h}$:

$$\langle F\rangle_B\sim r_0 W F_0(\overline{h}). \tag{A3}$$

Minimization leads to the second scaling relation:

$$\frac{h_m}{\overline{h}}\sim\frac{\overline{h}}{h_0}. \tag{A4}$$

The treatment of the other scaling regimes is given in Appendix B, along with the case of systems bound by pressure, and the full results are presented in Fig. 4 and Table I.

APPENDIX B: TWO-DIMENSIONAL SCALING

In this appendix we outline the arguments leading to the scaling relations summarized in Fig. 4 and Table I. Using the conelike profile approximation for the membrane in region A of Fig. 2:

$$h(\vec{r})=h_0+\alpha(|\vec{r}|-r_0),$$

we can integrate the free energy in this region. The only significant term in this region is that of the Helfrich repulsion and therefore the energy density in this region is

$$\langle F\rangle_A\propto\left(\frac{T^2}{\kappa\alpha^2}\right)\left[\ln\frac{h_m}{h_0}-(r_0\alpha-h_0)\left(\frac{1}{h_m}-\frac{1}{h_0}\right)\right]. \tag{B1}$$

We add this free energy to that of region B which was calculated in Sec. II for systems bound by pressure and in Appendix A for systems bound by attractions [Eqs. (2.3) and (A1)]. *A priori* the sum of these two terms has four regimes corresponding to the different limits:

$$\ln(h_m/h_0)\ll\frac{r_0\alpha}{h_0} \quad \text{and} \quad r_0\gg R, \tag{B2a}$$

$$\ln(h_m/h_0)\ll\frac{r_0\alpha}{h_0} \quad \text{and} \quad r_0\ll R, \tag{B2b}$$

$$\ln(h_m/h_0)\gg\frac{r_0\alpha}{h_0} \quad \text{and} \quad r_0\ll R, \tag{B2c}$$

$$\ln(h_m/h_0)\gg\frac{r_0\alpha}{h_0} \quad \text{and} \quad r_0\gg R. \tag{B2d}$$

However, not all four limits are accessible because there are interdependencies that must be consistent. We find three consistent limits while the fourth, corresponding to

$$\ln\frac{h_m}{h_0}\gg\frac{r_0\alpha}{h_0} \quad \text{and} \quad r_0\gg R, \tag{B3}$$

is inconsistent with the scaling laws applied to h_m and R. ($R\sim W$, which is the horizontal length scale.)

Minimization of the total free energy [Eq. (B1) and Eqs. (2.3) and (A1)] leads to the final scaling relations for h_m which are summarized in Table I and Fig. 4. (Note that the scaling relation for W is not dependent on the above mentioned regimes, only on the type of binding interaction.)

[1] R. M. Servuss and W. Helfrich, J. Phys. (France) (France) **50**, 809 (1989); U. Seifert and R. Lipowsky, Phys. Rev. A **42**, 4768 (1990); J. Rädler and E. Sackmann, J. Phys. (France) II **3**, 727 (1993).

[2] G. I. Bell, Science **200**, 618 (1978); E. A. Evans, Biophys. J. **48**, 175 (1985); **48**, 185 (1985).

[3] Ernst-Ludwig Florin, Vincent T. Moy, and Hermann E. Gaub, Science **264**, 415 (1994).

[4] R. Bruinsma, M. Goulian, and P. Pincus, Biophys. J. **67**, 756 (1994); D. Zuckerman and R. Bruinsma, Phys. Rev. Lett. **74**, 3900 (1995).

[5] R. Lipowsky and S. Leibler, Phys. Rev. Lett. **56**, 2541 (1986); R. Lipowsky Nature (London) **349**, 475 (1991); Phys. Rev. Lett. **77**, 1652 (1996).

[6] M. Mutz and W. Helfrich, Phys. Rev. Lett. **62**, 2881 (1989).

[7] R. Bar-Ziv, R. Menes, E. Moses, and S. A. Safran, Phys. Rev. Lett. **75**, 3356 (1995).

[8] G. I. Bell, M. Dembo, and P. Bongrand, Biophys. J. **45**, 1051 (1984); J. Braun, J. R. Abney, and J. C. Owicki, Nature (London) **310**, 316 (1984).

[9] E. A. Evans, Biophys. J. **48**, 175 (1985).

[10] N. Dan, P. Pincus, and S. A. Safran, Langmuir **9**, 2768 (1993); N. Dan, A. Berman, P. Pincus, and S. A. Safran, J. Phys. (France) II (France) II **4**, 1713 (1994).

[11] R. Menes and S. A. Safran (unpublished).

[12] Roland R. Netz, J. Phys. (France) (to be published).

[13] P. B. Canham, J. Theor. Biol. **26**, 61 (1970); W. Helfrich, Z. Naturforsch. C **28**, 693 (1973).

[14] S. A. Safran, *Statistical Thermodynamics of Surfaces, Interfaces and Membranes* (Addison-Wesley, Reading, MA, 1994).
[15] R. Lipowsky, Phys. Rev. B **32**, 1731 (1985).
[16] W. Helfrich, Z. Naturforsch. A **33**, 305 (1977).
[17] When $\vec{\nabla} h \sim 1$ the curvature approximation used here breaks down. However, one can show that the profile slope near the pinning site scales as $\sqrt{k_B T/\kappa}$, and that for experimental membranes ($\kappa \simeq 15 k_B T$) the approximation breaks down only at $h_0 \overline{h} \sim 10^{-3}$.
[18] In systems dominated by surface tension the gradient term in the free energy has the form $\gamma(\nabla h(x))^2$, and the profiles that minimize this free energy are monotonic. In the linear regime where the pinning is very weak we can linearize the interactions to find that the second order linear Euler-Lagrange equation is solved by exponentially decaying modes.
[19] In the laser experiment one could observe in the overshoot region curvature fluctuations which indicate that there is no massive tension buildup in this structure.
[20] M. Goulian, R. Bruinsma, and P. Pincus, Europhys. Lett. **22**, 145 (1993).
[21] J. N. Israelachvili, *Intermolecular and Surface Forces* (Academic, New York, 1985).
[22] S. T. Milner and D. Roux, J. Phys. (France) I **2**, 1741 (1992); P. G. DeGennes, *Scaling Concepts in Polymer Physics* (Cornell University Press, Ithaca, 1979).
[23] R. Lipowsky, Europhys. Lett. **7**, 255 (1988).